Calculating Molecular Polarizabilities using

Exact Frozen Density Embedding with

External Orthogonality

Gaohe Hu, Pengchong Liu, and Lasse Jensen*

Department of Chemistry, The Pennsylvania State University, 104 Benkovic Building, University Park, 16802, United States.

E-mail: jensen@chem.psu.edu

Abstract

Frozen Density Embedding(FDE) with freeze-and-thaw cycles is a formally exact embedding scheme. In practice, this method is limited to systems with small density overlaps when approximate non-additive kinetic energy functionals are used. It has been shown that the use of approximate non-additive kinetic energy functionals can be avoided when external orthogonality(EO) is enforced, and FDE can then generate exact results even for strongly overlapping subsystems. In this work, we present an implementation of exact FDEc-EO (coupled FDE TDDFT with EO) for the calculation of polarizabilities in the Amsterdam Density Functional program (ADF) package. EO is enforced using the level-shift projection operator method which ensures that orbitals between fragments are orthogonal. For pure-functionals we show that only the symmetric EO contributions to the induced density matrix is needed. This leads to a simplified implementation for the calculation of polarizability that can exactly reproduce supermolecular TDDFT results. We further discuss the limitation of exact FDEc-EO in interpreting subsystem polarizabilities due to the non-unique partitioning

of the total density. We show that this limitation is due to the fact that subsystem polarizabilities partitioning is dependent on how the subsystems are initially polarized. As supermolecular virtual orbitals are exactly reproduced, this dependence is attributed to the description of the occupied orbitals. In contrast, for excitations of subsystems that are localized within one subsystem, we show that the excitation energies are stable with respect to the orders of polarization. This observation shows that impacts from the non-unique nature of exact FDE on subsystem properties can be minimized by better fragmentation of the supermolecular systems if the property is localized. For global properties like polarizability, this is not the case, and non-uniqueness remains independent of the fragmentation used.

1 Introduction

Quantum embedding methods have seen great development over recent years. ^{1–7} In general, quantum embedding methods partition the total(supermolecular) system into multiple subsystems such that a divide-and-conquer strategy can be applied. Usually, the subsystems of interests are termed as the active subsystem and the remaining is known as the environment. Quantum embedding allows different levels of approximations to be applied to different subsystems. This leads to a common strategy that active subsystem with higher level theory is embedded into environment with lower level theory, which makes it affordable for calculations of large systems. Among embedding methods, quantum mechanical/molecular mechanics(QM/MM) is the most common one that has been applied to large biological systems such as enzymes catalysis and even RNA-protein complexes. ⁹ Other embedding methods aimed at higher accuracy including density matrix embedding ^{10–12} and Green's function embedding, ^{13–16} have been applied to descriptions of strongly correlated systems.

When Kohn-Sham density functional theory(KS-DFT) is applied to a quantum embedding method, it is known as subsystem DFT.⁶ Subsystem DFT directly partitions supermolecular electron density where each subsystem is treated using KS-DFT. Instead of direct

calculation of the supermolecular system, subsystem DFT is intended to solve KS equations with constrained electron density(KSCED) of each subsystem. ¹⁷ Within the framework of KS DFT, interactions between subsystems are described as an embedding potential term in the KS equation of each subsystem. Frozen density embedding(FDE), as a variant of subsystem DFT, solves the KSCED equation for the active subsystem while densities of the remaining subsystems are kept frozen. Self-consistent solution of the supermolecular density is achieved through freeze-and-thaw cycles where the roles of frozen and active subsystems are interchanged iteratively. Originally, FDE was introduced as a DFT-in-DFT embedding scheme where both the active subsystem and the environment are treated using DFT, ¹⁷ but the method have been extended to go beyond the accuracy of DFT or increase efficiency in dealing with large systems. To go beyond DFT level accuracy, methods that embeds higher-level theory such as correlated wavefunction ^{18–21} methods or many-body GW methods ²² have been developed. To gain efficiency in the environment density generation, one approach that has been taken is to embed active subsystem into a polarizable environment. ^{23–25}

FDE has also been generalized to excited state formulation within a linear response time-dependent DFT(TDDFT) framework. ^{26,27} Further work has been done to include frequency response of the environment, thus the coupling between the response of the environment and active subsystem is captured. ^{28–30} Recently, there have been efforts to implement real-time TDDFT within subsystem framework ^{31–35} which can provide information about excitation energy transfer and coupling between subsystems. Subsystem based methods(DFT-in-DFT and WF-in-DFT) have been widely applied for the analysis of interactions between environment and active subsystems. ^{27,36} For example, the solvatochromic shifts of excitation energies for molecules solvated by water molecules. ^{37,38} Another example is the application of subsystem methods to transition metal complexes ^{39–41} where the transition metal ions are treated as the active subsystem while the ligands are chosen as environment. Absorption of molecules on metal surfaces can also be modeled with subsystem based methods where the absorbed species and neighboring metal are treated as the active subsystem and the

remaining is the environment. 42,43

Subsystem DFT and FDE are formally equivalent to KS-DFT, however, in practice, the non-additive potentials present in embedding potential requires approximations. For the exchange-correlation(XC) part, the non-additive term is calculated in the same manner as approximate density functional in supermolecular DFT, unless hybrid XC functionals are used. Traditionally, kinetic energy density functionals are used to approximate the nonadditive kinetic potential (NAKP), however, due to its local nature, it has been shown to only be applicable to systems with weak density overlaps. 44,45 Although accurate NAKP can be generated with potential reconstruction methods 46,47 or the inverse Kohn-Sham method. 48 one can, alternatively, directly bypass NAKP by enforcing external orthogonality(EO) ^{49–51} among subsystem orbitals. We have previously reported an implementation of EO for both ground state FDE⁵¹ and excited state FDE⁵² by adopting a simple level-shift projection operator. ⁵³ By doing so, the kinetic energy of supermolecular system can be directly decomposed into sum of subsystem kinetic energies that are calculated with subsystem orbitals with EO. As demonstrated in previous work on ground state FDE, ⁵¹ when EO and supermolecular basis sets are combined, supermolecular KS-DFT results can be exactly reproduced. FDE with EO (FDE-EO) have also been extended to excited state properties using time-dependent density functional theory (TDDFT). 52,54,55 Due to a non-symmetric contribution from the EO response kernel, Neugebauer and coworkers have shown that a non-hermitian solver is necessary for obtained exact excitation energies and oscillator strengths. 54 Neugebauer and coworkers have also extended the approach to other response properties based on damped response theory. ⁵⁶

In this work, we present an implementation of coupled FDE TDDFT with (FDEc-EO) for the calculation of exact molecular polarizabilities within the Amsterdam Density Functional (ADF) program package. ^{57,58} EO is enforced using the level-shift projection operator method of Manby and co-workers. ^{53,59,60} Similar to ground state FDE, the approach starts with monomer subsystem KS orbitals and uses freeze-and-thaw cycles to generate converged

response properties. The method is benchmarked against supermolecular TDDFT as well as finite field differentiation of FDE-EO and is shown to exactly reproduce the KS-TDDFT results. Furthermore, we will discuss the non-uniqueness of the partitioning and show how this affects subsystem response properties.

2 Theory

Analogous to FDE for ground state where the density is partitioned into subsystem densities, in FDE TDDFT the electron density response is decomposed into subsystem contributions. ^{26,28} For subsystem I, we have

$$\delta \rho_I(\mathbf{r}, \omega) = \int \chi_I(\mathbf{r}, \mathbf{r}', \omega) \, \delta v_I^{\text{eff}}(\mathbf{r}', \omega) \, d\mathbf{r}'$$
(1)

that shows the first-order change of the electron density as the response to an effective perturbation potential δv_I^{eff} at frequency ω , with subsystem response function $\chi_I(\mathbf{r}, \mathbf{r}', \omega)$.

The effective potential can be further decomposed into the external potential and the induced electronic potential from the density response of all subsystems as 26,28

$$\delta v_I^{\text{eff}}(\mathbf{r}') = \delta v_I^{\text{ext}}(\mathbf{r}') + \delta v_I^{\text{el}}(\mathbf{r}') = \delta v_I^{\text{ext}}(\mathbf{r}') + \sum_J \int f(\mathbf{r}', \mathbf{r}'', \omega) \, \delta \rho_J(\mathbf{r}'', \omega) \, d\mathbf{r}''$$
 (2)

with the response kernel given by

$$f(\mathbf{r}', \mathbf{r}'', \omega) = \frac{1}{|\mathbf{r}' - \mathbf{r}''|} + \frac{\delta^2 E_{xc}[\rho]}{\delta \rho(\mathbf{r}') \delta \rho(\mathbf{r}'')} + \frac{\delta^2 T_s[\rho]}{\delta \rho(\mathbf{r}') \delta \rho(\mathbf{r}'')} - \frac{\delta^2 T_s[\rho_I]}{\delta \rho_I(\mathbf{r}') \delta \rho_I(\mathbf{r}'')} \delta_{IJ}$$
(3)

And the terms on the right-hand side correspond to the Coulomb potential, the XC potential and the last two terms constitute NAKP contributions. In the above equations, the adiabatic approximation has been adopted which assumes that f_{xc} is frequency-independent and that a local density approximation for the XC functional kernel is used.

The density response can be expressed in terms of orbital products as ⁶¹

$$\delta \rho_I(\mathbf{r}, \omega) = \sum_I \sum_{i, a \in I} \left[\delta P_{(ia)_I}(\omega) + \delta P_{(ai)_I}(\omega) \right] \phi_a^I(\mathbf{r}) \phi_i^I(\mathbf{r})$$
(4)

where we have taken the convention of using a, b, ... for virtual orbitals and i, j, ... for occupied orbitals. Occupied-virtual and virtual-occupied orbital transitions are distinguished explicitly with expansion coefficients $\delta P_{(ia)_I}$ and $\delta P_{(ai)_I}$. Although only intra-subsystem transitions are explicitly expressed here, inter-subsystem transitions are included implicitly since the same virtual orbital space is shared by all subsystems when supermolecular basis sets are used.

From Equation 2, the electronic potential can be expressed in terms of δP by introducing a coupling matrix \mathbf{K} with elements $K_{(ia)_I,(jb)_J}$: 61,62

$$K_{(ia)_I,(jb)_J} = \int d\mathbf{r} \int d\mathbf{r}' \phi_i^I(\mathbf{r}) \phi_a^I(\mathbf{r}) f(\mathbf{r}, \mathbf{r}', \omega) \phi_j^J(\mathbf{r}') \phi_b^J(\mathbf{r}')$$
(5)

such that

$$\delta v_{(ia)_I}^{\text{el}} = \sum_{jb \in J} \sum_{J} K_{(ia)_I,(jb)_J} \delta P_{(jb)_J}(\omega) + K_{(ia)_I,(bj)_J} \delta P_{(bj)_J}(\omega)$$
 (6)

where sum over J runs over all subsystems. When J = I, it corresponds to intra-subsystem coupling and when $J \neq I$ it corresponds to inter-subsystem coupling. The response of density matrix of subsystem I is then

$$\delta P_{(ia)_I}(\omega) = \chi^s_{(ia)_I} \left[\delta v^{\text{ext}}_{(ia)_I} + \sum_{jb \in J} \sum_J K_{(ia)_I,(jb)_J} \delta P_{(jb)_J}(\omega) + K_{(ia)_I,(bj)_J} \delta P_{(bj)_I}(\omega) \right]$$

$$= \chi^s_{(ia)_I} \left[\delta v^{\text{ext}}_{(ia)_I} + 2 \sum_J \sum_{jb} K_{(ia)_I,(jb)_J} \delta P_{(jb)_J}(\omega) \right]$$
(7)

where the symmetry of the density matrix can be used such that only occ-virt(or virt-occ) elements are needed. Without EO and NAKP contributions, when real orbitals and pure XC density functionals are used, the coupling matrix is of a symmetric structure such that

 $K_{(ia)_I,(bj)_J} = K_{(ia)_I,(jb)_J}$ which leads to $K_{(ia)_I,(jb)_J} \delta P_{(jb)_J}(\omega) = K_{(ia)_I,(bj)_J} \delta P_{(bj)_I}(\omega)$. This form of FDE TDDFT is termed as coupled FDE (FDEc) since coupling between subsystems is included. ^{28,29}

To eliminate the requirement for approximate NAKP, an EO term can be included. ^{52,54,55} As remarked in previous work on EO contributions to FDE TDDFT, for perfectly orthogonalized subsystem orbitals, the EO potential should vanish as overlap matrices between subsystems vanish. ⁵² However, in practice, the EO potential serves as a first order correction to the coupled response since subsystem orbitals are not perfectly orthogonalized. ⁵²

The EO contributions to $K_{(ia)_I,(jb)_J}$ and $K_{(ia)_I,(bj)_J}$ are

$$K_{(ia)_I,(jb)_J}^{\text{EO}} = \mu S_{ij}^{I,J} S_{ba}^{J,I}$$
 (8)

$$K_{(ia)_I,(bj)_J}^{\text{EO}} = \mu S_{ib}^{I,J} S_{ja}^{J,I}$$
 (9)

where $S^{I,J}_{ij}$ represents coupling matrix element between i orbital of subsystem I and j orbital of subsystem J, and μ is a level-shift parameter. In our previous implementation of EO contributions to FDE TDDFT, we assumed a symmetric structure of the coupling matrix with EO contributions, 52 which is in fact an approximation. As shown by Neugenbauer and co-workers 55 the correct treatment of the EO contribution leads to a set of non-Hermitian response equations that needs to be solved. This is similar to the case for functionals that include some fraction of Hartree-Fock exchange. However, since supermolecular basis sets are used, all subsystems share the same virtual orbital space, thus there is no overlap between any subsystem occupied orbitals and virtual orbitals, no matter if they belong to the same subsystem or not such that $S^{I,J}_{ib} = S^{J,I}_{ja} = 0$, which ensures that Equation 9 vanishes.

This asymmetric feature of the EO coupling matrix again makes it possible to include

EO in the coupling matrix of (7) as an additional term:

$$\delta P_{(ia)_I} = \chi^s_{(ia)_I} \left[\delta v^{\text{ext}}_{(ai)_I} + 2 \sum_{jb \in I} K_{(ia)_I,(jb)_I} \delta P_{(jb)_I} + \sum_{jb \in J} \left(2K_{(ia)_I,(jb)_J} \delta P_{(jb)_J} + \mu S^{I,J}_{ij} S^{J,I}_{ba} \delta P_{(jb)_J} \right) \right]$$
(10)

as long as only pure exchange correlation functionals are used. In a compact matrix form we have

$$\delta \mathbf{P}_{I} = \chi_{I}^{s} \left[\delta \mathbf{v}_{I}^{\text{ext}} + 2 \mathbf{K}_{II}^{\text{eff}} \delta \mathbf{P}_{I} + 2 \mathbf{K}_{IJ}^{\text{eff}} \delta \mathbf{P}_{J} + \delta \mathbf{v}_{I(J)}^{\text{EO}} \right]$$
(11)

where $\delta \mathbf{v}_{I(J)}^{\mathrm{EO}} \equiv \mu \mathbf{S}_{occ,occ}^{I,J} \mathbf{S}_{vir,vir}^{J,I} \delta \mathbf{P}_{J}$ and the symmetric structure of the conventional coupling matrix is preserved. In this way, we have correctly included the EO contribution to inter-subsystem coupling and both intra- and inter-subsystem couplings can all be described correctly. This form of FDE TDDFT with EO is thus termed as FDEc-EO.

As for the initial guess, an approximate version of FDE TDDFT can be performed. By neglecting all inter-subsystem coupling, uncoupled FDE TDDFT(FDEu) considers only \mathbf{K}_{II} such that

$$\delta \mathbf{P}_{I} = \chi_{I}^{s} \left[\delta \mathbf{v}_{I}^{\text{ext}} + 2 \mathbf{K}_{II} \delta \mathbf{P}_{I} \right]$$
 (12)

After convergence is reached for Equation 11, supermolecular polarizability can be expressed as a summation of subsystem polarizabilities

$$\alpha_{\lambda\nu} = \sum_{I} \alpha_{\lambda\nu}^{I}$$

$$= \sum_{I} \sum_{(ia)_{I}} 2H_{(ia)_{I}}^{\lambda} \delta P_{(ia)_{I}}^{\nu}$$
(13)

where $\lambda, \nu = x, y, z$ and $H_{(ia)_I}$ is the elements of the dipole matrix for subsystem I. For completeness the non-Hermitian TDDFT solver⁵⁵ for calculating excitation energies was also implemented into the ADF program.

3 Methods

All calculations were carried out with a local modified version of ADF2021, 57,58 and a Vosko-Wilk-Nair (VWN) 63 form of local density approximation (LDA) XC potential were used. The triple- ζ with one polarization function (TZP) 64 basis set from ADF basis set library was used for all systems. Geometry optimizations of all monomers and decanal were also carried out under the same basis set and XC functional. Thomas-Fermi kinetic energy density functional approximation 65 was used to evaluate NAKP for conventional FDE calculations.

For all external orthogonality calculation, the subsystem orbitals are orthogonalized with a level-shift parameter μ . As suggested in previous work, 51,52 a level-shift parameter of 10^6 E_h is large enough to enforce external orthogonality among fragment orbitals, while $> 10^7$ E_h may lead to numerical instabilities. 53 Thus, throughout this work, $\mu = 10^6$ E_h is used for all FDE with EO calculations. Implementation of FDEc-EO is based on subresponse module of ADF. 29 To demonstrate the exactness of FDEc-EO calculation of polarizability, an accurate density fitting is necessary, therefore, ZlmFit 66 scheme for density fitting has also been implemented for subresponse module of ADF. Static supermolecular polarizabilities were also calculated with both TDDFT and finite differentiation of ground dipole moments as benchmark. For the finite differentiation calculation of polarizabilities, derivatives of molecular dipole moments based on ground state FDE EO with respect to external electric fields are calculated with two-point differentiation.

A typical workflow for FDEc-EO polarizability calculation is: 1) Ground state calculation of each subsystem with supermolecular basis sets; 2) FDE freeze-and-thaw cycles on one subsystem followed by a FDEu response calculation; 3) One FDEu response calculation on all the other subsystems; 4) Use results from step 2 and 3 as input for a FDEc response calculation.

4 Results and Discussion

4.1 Polarizability with FDEc-EO

To demonstrate that FDEc-EO can exactly reproduce the supermolecular polarizability, the static polarizabilities of benzene dimer systems are calculated. The dimer systems are set up such that two benzene molecules are placed face to face and each molecule corresponds to one subsystem. They are separated along z-axis from 3.18 Å to 5.28 Å and polarizabilities of each separation distance are calculated. Other smaller systems, including helium dimer, FHF⁻ and C₂H₆ are also benchmarked in the same manner and shown in the Supporting Information.

In Figure 1 polarizabilities and absolute errors of the Benzene dimer systems with respect to separation distances are shown. Static polarizability of these systems is obtained in four different ways, namely supermolecular linear response (KS), finite difference of molecular dipole moments (FD), FDEc with EO (FDEc-EO) and FDEc without EO (FDEc-noEO). All of FD, FDEc-EO and FDEc-noEO are based on the same converged supermolecular density from FDE freeze-and-thaw cycles. Both FDEc-EO and FDEc-noEO are based on the same FDEu results, the only difference is that in FDEc-noEO, the EO term is excluded from the response kernel, thus the EO contribution to the induced potential is removed.

As shown in Figure 1, all three methods are benchmarked against KS results and the absolute error is plotted. In general, both FD and FDEc-EO results agree very well with KS results, while FDEc-noEO tends to only be accurate as the monomers are well separated.

Since FD calculation takes the derivatives with respect to the external electric field and it is based on exact FDE ground state results, all errors of FD results are introduced by numerical errors from finite differentiation. Since symmetry is not enforced in the calculations, small differences between α_{xx} and α_{yy} components are found. In principle, tighter numerical settings should eliminate this difference, however, it was not pursued here. As shown in Figure 1, at all separation distances, FDEc-EO results are significantly more accurate than

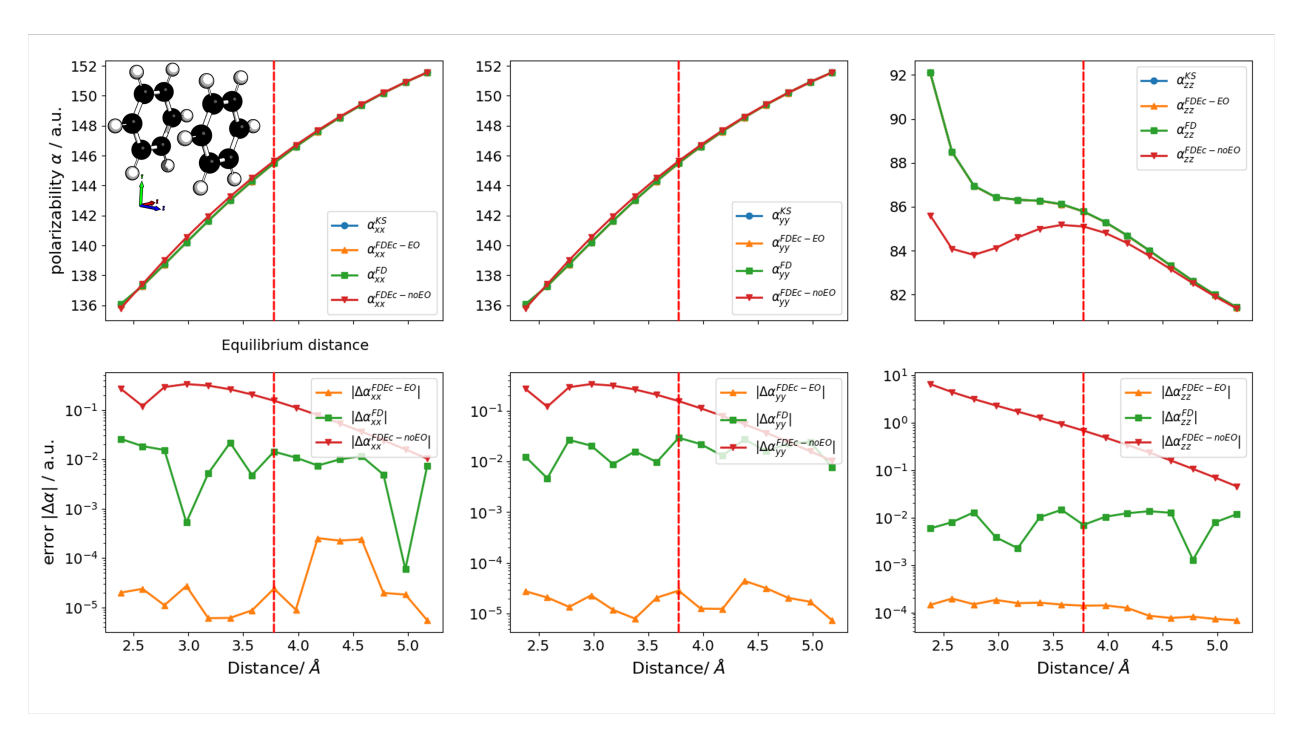


Figure 1: Polarizability and absolute errors with respect to separation distances between two Benzene molecules along z-axis. The equilibrium separation distance is marked with red dashed line.

those of FD. To be specific, the errors of α_{xx} and α_{yy} are oscillating around 10^{-5} , while errors of α_{zz} are around 10^{-4} which is slightly larger than those of the other two components. Because the dimer systems are separated along z-axis, overlaps between subsystems are strongest along z direction comparing to x and y directions. Since a level-shift factor of $10^6 E_h$ is used, numerical errors of overlap matrix will also be shifted significantly. Therefore, deviations from KS results are largest for α_{zz} component due to errors from overlaps between subsystems. As demonstrated recently by Neugebauer and coworkers, 54,55 a combination of supermolecular basis sets and EO makes sure the same virtual orbital space is shared by both subsystems which is necessary for exact description for inter-subsystem charger-transfer excitations. Meanwhile, enforcing EO between subsystems also avoids the failure of approximate NAKE in strongly-overlapping systems such as covalent bonded subsystems(see Supporting Information).

In addition to the benzene dimer systems, helium dimer systems separated by different

distances are shown in the Supporting Information, of which KS supermolecular polarizabilities at all distances can be exactly reproduced with the same numerical settings shown in previous section. Other molecular systems, namely water dimer, FHF⁻ and C₂H₆, are also shown to test the ability of FDEc-EO in describing interactions of different strength between subsystems, which covers the cases from weak hydrogen bond to strong hydrogen bond and finally covalent bond. For all interactions of different strength, FDEc-EO can exactly reproduce KS polarizabilities.

Besides results of FDEc-EO, FDEc-noEO results are also shown in Figure 1 to highlight the contribution of EO term to supermolecular response. At all distances, FDEc-noEO results exhibits very large errors comparing to those from FDEc-EO. It is only at the long-distance limit that the accuracy of FDEc-noEO becomes comparable to FD. Similar to those results from FDEc-EO, the errors are always larger for α_{zz} than both α_{xx} and α_{yy} . For α_{zz} , the error decreases as the overlap between the two subsystems decreases. Note that even at equilibrium distance, which represents moderate overlaps between subsystems, deviation of α_{zz} is also as large as 0.68 a.u comparing to the supermolecular TDDFT results. This indicates that even with EO orbitals, the contribution of EO term in response kernel is still important and cannot be neglected.

In contrast to our previous work on FDEc-EO,⁵² the current implementation includes a more accurate density fitting method which in addition to accounting for the full symmetry of the EO contribution is necessary to reproduce the supermolecular response properties. Based on discussions above, we can conclude that the current implementation of FDEc-EO can exactly reproduce supermolecular polarizabilities.

4.2 Non-uniqueness in subsystem polarization

One of the main advantageous of the FDE approach is the ability of calculating subsystem polarizabilities. As shown above the sum of subsystem polarizabilities can exactly reproduce the total supermolecular response. However, in the following we will show that the

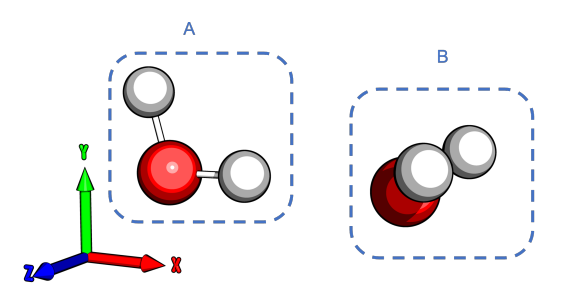


Figure 2: Water dimer system, each monomer corresponds to one subsystem

interpretation of subsystem polarizabilities is limited due to problems with non-unique nature of exact FDE method. ^{5,67–69} In our case, the problem of non-uniqueness emerges as the partitioning of subsystem polarizabilities is dependent on the order of polarization. While the subsystem polarizabilities obviously should depend on the nature of the fragments, i.e. which nuclei and how many electrons assigned to each fragment, it should ideally not depend on how that fragment has been polarized during the freeze-thaw cycles.

Table 1: Subsystem polarizabilities calculated with both FDEc-EO and FDE-TF with different orders of polarization.

Method	Initial Fragment	Polarizability/ a.u.					
		${\bf fragment} {\bf A}$			fragment B		
		α_{xx}	α_{yy}	α_{zz}	α_{xx}	α_{yy}	α_{zz}
FDEc-EO	A	10.44	7.70	8.67	10.74	8.76	8.08
	В	9.62	8.83	8.14	11.56	7.62	8.61
FDE-TF	A	10.34	8.07	8.66	10.02	8.43	8.04
	В	10.34	8.06	8.66	10.02	8.43	8.04

To demonstrate the polarization dependence and the possible origin of this dependence, a water dimer system has been studied as shown in Figure 2. Water dimer system was chosen because the overlap between the two monomers is weak enough so that Thomas-Fermi kinetic energy functional can give qualitatively correct results.⁵¹ Since exact FDE

would give non-unique results, while approximate FDE can give unique results, ^{67,68} polarizabilities and electron density calculated with FDE-TF are thus used for comparison. First, both supermolecular and subsystem polarizabilities calculated with exact FDE(FDEc-EO) and approximate FDE with Thomas-Fermi kinetic energy density functional(FDE-TF) in different orders of polarization are shown in Table 1. We then address the origin of the non-uniqueness problem by analyzing the polarized electron density in freeze-and-thaw cycles as shown in Figure 3.

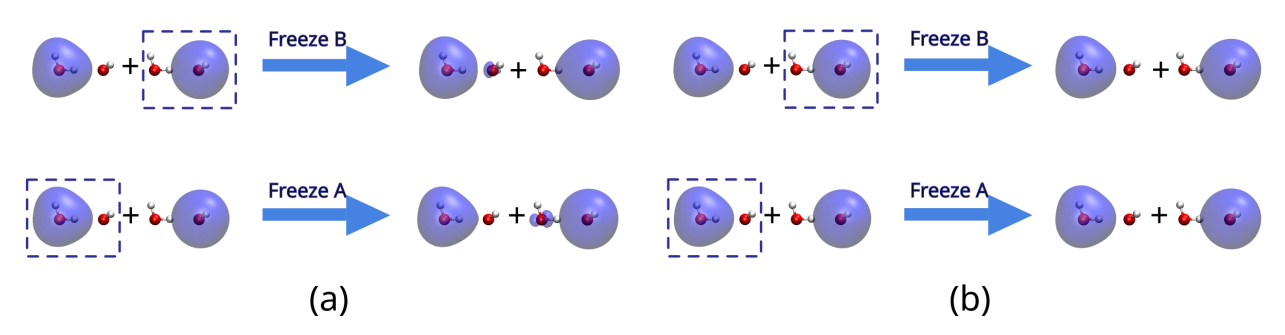


Figure 3: Electron density of each subsystem calculated with (a) FDE-EO and (b) FDE-TF. The arrows start from the initial fragment densities and point to the sets of electron densities of each subsystem.

In freeze-and-thaw cycles for ground state FDE-EO calculations, there is always one subsystem set as the initial subsystem to be polarized by the other initial active fragment. In our calculations, we have observed that for those two water monomers, the subsystem polarizabilities results are dependent on which monomer is chosen as the initial active fragment. In these cases two sets of subsystem polarizabilities partitioning are generated for the two orders of polarization. In Table 1 subsystem polarizabilities corresponding to different methods and different orders of polarization are shown. For FDE-TF, a Thomas-Fermi kinetic energy functional is used for NAKE, and the polarizabilities are calculated as a finite differentiation of molecular dipole moment with respect to an external electric field. For FDEc-EO, a regular FDEc-EO process is taken. Initial fragment refers to the fragment which is allowed to relax in the first freeze-and-thaw cycle while the other is frozen as the environment. Thus with different initial fragments, we have adopted different orders of polarization of the

subsystems.

As can be found from Table 1, for results calculated with FDE-TF, all components of polarizabilities of each subsystem stay almost invariant with respect to the different orders of polarization. While for FDEc-EO, supermolecular polarizability can be exactly reproduced with either fragment as initial fragment, but there is significant difference between subsystem polarizabilities. For instance, difference in α_{xx} of FDEc-EO can be around 0.8 a.u.(8%), while difference in α_{xx} of FDE-TF is only around 0.001 a.u.(0.01%). This indicates that when different orders of polarization are used, different subsystem polarizability partitioning is also expected in exact FDE while approximate FDE is not affected and can be regarded as invariant in practice. Such difference in subsystem polarizability partitioning hinders our further understanding of interactions between subsystems. As shown here, subsystem polarizabilities for both subsystems are determined by the orders of polarization and neither can be regarded as the correct one. Applications of exact FDE method are consequently limited because direct interpretation on subsystem polarizabilities would be impossible.

As has been pointed out in previous work, FDE is known to be formally non-unique. 5 The non-uniqueness is a consequence of lack of constraints on subsystem densities, as long as subsystem densities can sum up to supermolecular density, any sets of subsystem densities that are v-representable can be solutions to the KSCED equations. Non-uniqueness of subsystem densities can thus lead to other non-unique subsystem properties such as dipole moment and consequently subsystem polarizability. A variety of solutions to ensure uniqueness of embedding potential have also been proposed. $^{68,70-73}$ Although subtle differences are present, they share the idea that uniqueness is achieved by adding extra constraints to generate embedding potentials shared across all subsystems. By enforcing EO, we only remove the requirements for NAKE in embedding potential, and no extra constraints on embedding potential are applied. As for approximate FDE, since the errors introduced by approximate NAKE are minimized during freeze-and-thaw cycles, unique subsystem densities can be generated. 67

To understand why orders of polarization matter in exact FDE, we went back to analyze how the electron density gets polarized in the ground state. In Figure 3, electron densities of unpolarized subsystems and polarized in the first iteration of freeze-and-thaw cycles are shown, respectively. Although electron densities do get relaxed in the following freeze-and-thaw cycles, the majority of the electronic polarization is determined in the first iteration.

For subsystem densities calculated with FDE-TF, no significant difference is found for both orders of polarization. This agrees with the fact that approximate NAKE would generate unique solutions. As for subsystem densities calculated with FDE-EO, two sets of subsystem densities are generated when each subsystem is chosen as the initial one. To be more specific, when one fragment is allowed to relax in the first iteration, subsystem electron density gets polarized into the frozen environment. To enforce EO, supermolecular basis sets are used for FDE-EO calculations which accounts for electron delocalization into the inactive fragments. In the following thaw process of the frozen fragment in the first cycle, no subsystem electron density gets polarized into the environment. And such difference in the subsystem electron densities remain in the following cycles which results in two sets of subsystem densities. Note that electronic polarization from the active fragment into the inactive fragment is not the same as charge spill-out in approximate FDE which is attributed to lack of repulsion from approximate NAKE.

To conclude, exact FDE with EO does not change the non-unique nature of FDE method and it leads to limited ability to interpret subsystem properties. In our implementation of FDEc-EO, direct decomposition of the supermolecular polarizability into subsystem polarizabilities is thus also non-unique, which results in different sets of subsystem polarizabilities and therefore one has to be careful to assign physical significance.

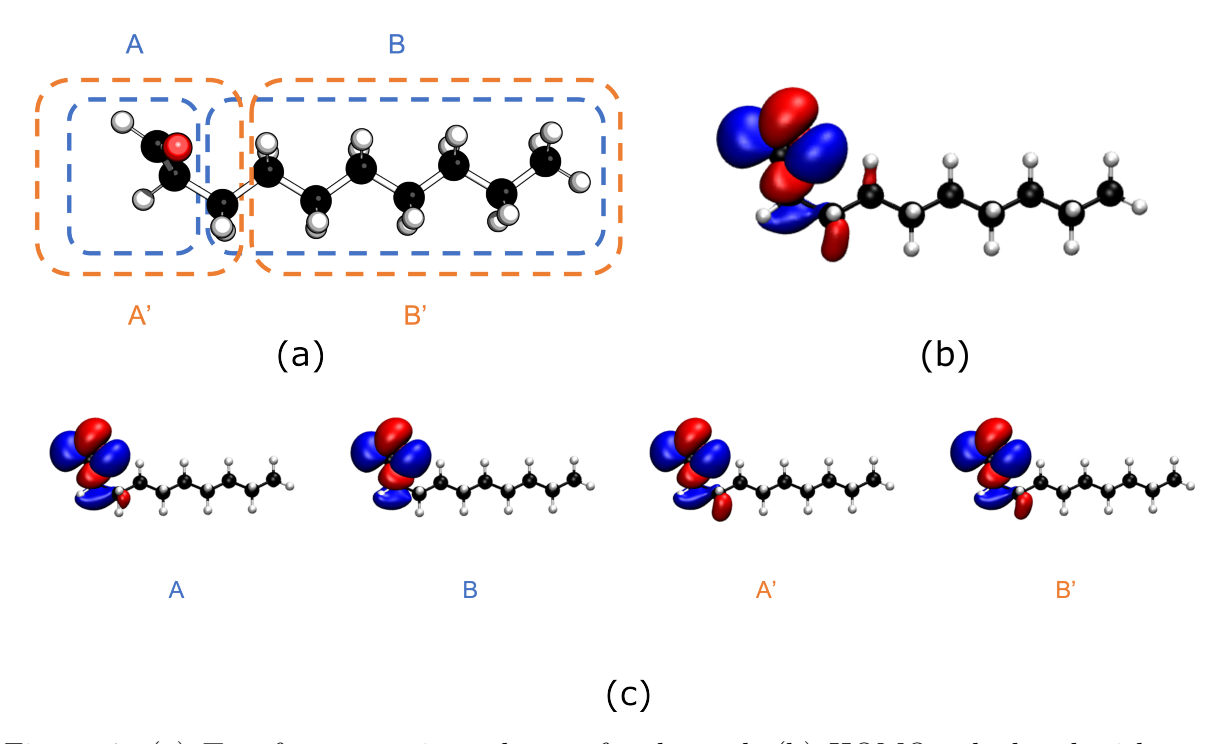


Figure 4: (a) Two fragmentation schemes for decanal; (b) HOMO calculated with supermolecular DFT; (c) HOMOs calculated with FDE-EO and the label indicates the initial active fragments.

Table 2: FDEu excitation energies of decanal that corresponds to the HOMO to LUMO transition.

Initial Fragment	Excitation energy/ eV				
\mathbf{A}	4.19				
В	4.29				
\mathbf{A}'	4.18				
\mathbf{B}'	4.20				
Supermolecular	4.16				

4.3 Fragmentation of Supermolecular System and Localized Excitation

Although different orders of polarization in exact FDE freeze-and-thaw calculations may results in different partitioning of supermolecular properties, we expect that properties that are localized within only one subsystem should stay robust with respect to different polarization orders. An example of this would be excitation energies localized to one fragment. Previous work have shown that the excitation energies depends on the specific approach used to ensure EO.⁷⁴ Here we will examine the dependence on the polarization order. We show an example of decanal molecule shown in Figure 4(a) where there is a supermolecular HOMO localized on the aldehyde group and neighboring carbon atoms as shown in Figure 4(b).

To illustrate how localization of the orbitals affect the results, two different fragmentation are shown in Figure 4(a). Those two fragmentation schemes, denoted as AB and A'B', differs in how many neighboring carbon atoms are included together with aldehyde group in one fragment. And this leads to different portions of supermolecular HOMO localized in one fragment. With different fragments as initial fragments, due to the non-unique problem stated in previous section, different excitation energies are expected. In Table 2, we have shown the excitation energies calculated with FDEu for both orders of polarization and both fragmentation schemes. As a reference, supermolecular excitation energy for the same HOMO to LUMO transition is also shown. Since FDEu cannot fully capture inter-subsystem coupling, the excitation energy cannot exactly reproduce the supermolecular results. However, we can still observe significant difference when different orders of polarization is applied. In AB fragmentation, the difference is around 0.1 eV, while in A'B' the difference is 0.02 eV. Such improvement on stability of excitation energy can be justified by the HOMO of the supermolecular system. As can be found in Figure 4(c), where the HOMOs of the subsystems to the aldehyde group ends are plotted. Note that since exact FDE can reproduce supermolecular virtual orbitals no matter how the fragmentations are performed, only difference is the quality of the occupied orbitals. As stated before, the supermolecular HOMO from KS DFT is localized within the aldehyde and closest carbon atoms, thus A'B' fragmentation which could describe the HOMO more precisely gives more stable results. This idea is supported by data from Figure 4(c). In A'B', the difference between the HOMO generated in both orders of polarization agree with each other better than those from AB. This is also consistent with previous work demonstrating that the best results were obtained for embedding in which the subsystem HOMO best resembled that of the supermolecular system. ⁷⁴ It is worth noticing that although only the carbon atom closest to aldehyde group is included in fragment A, part of the HOMO is delocalized on the carbon atom next to it. Such delocalization of occupied orbital, again, is a result of supermolecular basis sets. As for A'B', both orders of polarization give similar HOMO, which indicates that the excitation localized within the fragment is better described.

We also compared subsystem polarizabilities with different orders of polarization. Under both fragmentation schemes, the partitioning of the subsystem polarizability is depending on the order of polarization, while the supermolecular polarizability always remain robust. As shown in Table 3, deviations from the supermolecular results remain around 1% and is independent on the order of polarization. In contrast, the two set of subsystem polarizabilities are significantly different. When comparing results from AB and A'B' fragmentation, it can be found that the relative magnitudes of subsystem polarizabilities is reversed, while the difference between subsystem polarizabilities of the two orders of polarization is similar. Thus, extending the fragments does not mitigate the non-uniqueness of the subsystem polarizabilities. One probable explanation of such difference is that unlike excitation between localized orbitals, the polarizability involves numerous transitions from occupied orbitals that are delocalized over multiple subsystems to virtual orbitals.

Table 3: Subsystem polarizabilities of decanal calculated for two orders of polarization of two fragmentation schemes.

Initial Fragment	Polarizability/ a.u. Subsystem A Subsystem B						
	α_{xx}	α_{yy}	α_{zz}	α_{xx}	α_{yy}	α_{zz}	
A	48.04	24.60	33.01	116.51	90.05	82.69	
В	32.14	21.87	31.47	132.41	92.78	84.24	
	Sub	systen	ı A' Sub		$\overline{\text{system B}'}$		
	α_{xx}	α_{yy}	α_{zz}	α_{xx}	α_{yy}	α_{zz}	
\mathbf{A}'	63.25	36.56	43.04	101.29	78.10	72.66	
\mathbf{B}'	47.60	33.38	41.63	116.96	81.28	74.07	
Supermolecular polarizability	α_{xx}		α_{yy}		α_{zz}		
Supermolecular polarizability	164.56		114.66		115.70		

5 Conclusions

In this work, we present an implementation of FDEc-EO for the calculation of exact polarizabilities in the Amsterdam Density Functional program (ADF) package. Comparing to supermolecular TDDFT, there is no more approximation introduced (although both require approximate XC functionals), such implementation is thus exact comparing to supermolecular TDDFT. To avoid using a NAKP, we adapt EO through a level-shift projection operator method, which ensures that orbitals between fragments are orthogonal. We show that for pure-functionals only the symmetric EO contributions to the induced density matrix is needed which this leads to a simplified implementation for calculation of polarizability that can exactly reproduce supermolecular TDDFT results. To test the accuracy of this method, we have shown example systems with different strengths of inter-subsystem couplings. Comparing to supermolecular TDDFT, the supermolecular polarizabilities obtained with our implementation of FDEc-EO is exact. We further investigate the non-unique subsystem polarizability partitioning which is a result of differences in electronic polarization process in freeze-and-thaw cycles and roots in the non-unique nature of exact FDE. The subsystem polarizability partitioning limits further applications of such method on analysis

of subsystem interactions. While the non-uniqueness problem could not be solved within current framework, we also test the applicability of FDEu on localized properties. We show that for excitations involving localized orbitals, FDEu is invariant with respect to different orders of polarization while properties involving delocalized transitions such as subsystem polarizability can not be correctly described. In general, this formulation could be used as a benchmark for further development in approximate FDE methods.

Acknowledgments

The authors gratefully acknowledge financial support from DE-SC0018038, National Science Foundation Grant CHE-1856419 and CHE-2312222. Simulations in this work were in part performed on the Pennsylvania State University's Institute for Computational and Data Sciences' Roar supercomputer (https://icds.psu.edu/).

Supplementary Information

The supplementary information contains additional comparisons between supermolecular TDDFT and FDE-EO polarizabilities for He-dimer, water-dimer, FHF⁻, and C₂H₆.

References

- (1) Gordon, M. S.; Fedorov, D. G.; Pruitt, S. R.; Slipchenko, L. V. Fragmentation Methods: A Route to Accurate Calculations on Large Systems. *Chem. Rev.* **2012**, *112*, 632–672.
- (2) Jones, L. O.; Mosquera, M. A.; Schatz, G. C.; Ratner, M. A. Embedding Methods for Quantum Chemistry: Applications from Materials to Life Sciences. J. Am. Chem. Soc. 2020, 142, 3281–3295.

- (3) Goez, A.; Neugebauer, J. In *Frontiers of Quantum Chemistry*; Wójcik, M. J., Nakatsuji, H., Kirtman, B., Ozaki, Y., Eds.; Springer Singapore: Singapore, 2018; pp 139–179.
- (4) Sun, Q.; Chan, G. K.-L. Quantum Embedding Theories. Acc. Chem. Res. 2016, 49, 2705–2712.
- (5) Krishtal, A.; Sinha, D.; Genova, A.; Pavanello, M. Subsystem Density-Functional Theory as an Effective Tool for Modeling Ground and Excited States, Their Dynamics and Many-Body Interactions. J. Phys.: Condens. Matter 2015, 27, 183202.
- (6) Jacob, C. R.; Neugebauer, J. Subsystem Density-Functional Theory. Wires Comput. Mol. Sci. 2014, 4, 325–362.
- (7) Gomes, A. S. P.; Jacob, C. R. Quantum-Chemical Embedding Methods for Treating Local Electronic Excitations in Complex Chemical Systems. Annu. Rep. Prog. Chem., Sect. C: Phys. Chem. 2012, 108, 222–277.
- (8) Senn, H. M.; Thiel, W. QM/MM Studies of Enzymes. Curr. Opin. Chem. Biol. 2007, 11, 182–187.
- (9) Pokorná, P.; Kruse, H.; Krepl, M.; Šponer, J. QM/MM Calculations on Protein–RNA Complexes: Understanding Limitations of Classical MD Simulations and Search for Reliable Cost-Effective QM Methods. J. Chem. Theory Comput. 2018, 14, 5419–5433.
- (10) Knizia, G.; Chan, G. K.-L. Density Matrix Embedding: A Strong-Coupling Quantum Embedding Theory. J. Chem. Theory Comput. 2013, 9, 1428–1432.
- (11) Wouters, S.; Jiménez-Hoyos, C. A.; Sun, Q.; Chan, G. K.-L. A Practical Guide to Density Matrix Embedding Theory in Quantum Chemistry. J. Chem. Theory Comput. 2016, 12, 2706–2719.
- (12) Knizia, G.; Chan, G. K.-L. Density Matrix Embedding: A Simple Alternative to Dynamical Mean-Field Theory. *Phys. Rev. Lett.* **2012**, *109*, 186404.

- (13) Zgid, D.; Chan, G. K.-L. Dynamical Mean-Field Theory from a Quantum Chemical Perspective. J. Chem. Phys. **2011**, 134, 094115.
- (14) Chibani, W.; Ren, X.; Scheffler, M.; Rinke, P. Self-Consistent Green's Function Embedding for Advanced Electronic Structure Methods Based on a Dynamical Mean-Field Concept. Phys. Rev. B 2016, 93, 165106.
- (15) Rusakov, A. A.; Iskakov, S.; Tran, L. N.; Zgid, D. Self-Energy Embedding Theory (SEET) for Periodic Systems. *J. Chem. Theory Comput.* **2019**, *15*, 229–240.
- (16) Onida, G.; Reining, L.; Rubio, A. Electronic Excitations: Density-Functional versus Many-Body Green's-Function Approaches. *Rev. Mod. Phys.* **2002**, *74*, 601–659.
- (17) Wesolowski, T. A.; Warshel, A. Frozen density functional approach for ab initio calculations of solvated molecules. *J. Phys. Chem.* **1993**, *97*, 8050–8053.
- (18) Huang, P.; Carter, E. A. Self-Consistent Embedding Theory for Locally Correlated Configuration Interaction Wave Functions in Condensed Matter. J. Chem. Phys. 2006, 125, 084102.
- (19) Govind, N.; Wang, Y.; da Silva, A.; Carter, E. Accurate Ab Initio Energetics of Extended Systems via Explicit Correlation Embedded in a Density Functional Environment. *Chem. Phys. Lett.* **1998**, *295*, 129.
- (20) Govind, N.; Wang, Y. A.; Carter, E. A. Electronic-Structure Calculations by First-Principles Density-Based Embedding of Explicitly Correlated Systems. J. Chem. Phys. 1999, 110, 7677.
- (21) Wesołowski, T. A. Embedding a Multideterminantal Wave Function in an Orbital-Free Environment. *Phys. Rev. A* **2008**, *77*, 012504.
- (22) Tölle, J.; Deilmann, T.; Rohlfing, M.; Neugebauer, J. Subsystem-Based GW/Bethe-Salpeter Equation. J. Chem. Theory Comput. **2021**, 17, 2186–2199.

- (23) Pal, P. P.; Liu, P.; Jensen, L. Polarizable Frozen Density Embedding with External Orthogonalization. *J. Chem. Theory Comput.* **2019**, *15*, 6588–6596.
- (24) Egidi, F.; Angelico, S.; Lafiosca, P.; Giovannini, T.; Cappelli, C. A Polarizable Three-Layer Frozen Density Embedding/Molecular Mechanics Approach. J. Chem. Phys. 2021, 154, 164107.
- (25) Harshan, A. K.; Bronson, M. J.; Jensen, L. Local-Field Effects in Linear Response Properties within a Polarizable Frozen Density Embedding Method. J. Chem. Theory Comput. 2022, 18, 380–393.
- (26) Casida, M. E.; Wesolowski, T. A. Generalization of the Kohn-Sham Equations with Constrained Electron Density Formalism and its Time-Dependent Response Theory Formulation. *Int. J. Quantum Chem.* **2004**, *96*, 577–588.
- (27) Wesolowski, T. A. Hydrogen-Bonding-Induced Shifts of the Excitation Energies in Nucleic Acid Bases: An Interplay between Electrostatic and Electron Density Overlap Effects. J. Am. Chem. Soc. 2004, 126, 11444–11445.
- (28) Neugebauer, J. Couplings between electronic transitions in a subsystem formulation of time-dependent density functional theory. J. Chem. Phys. 2007, 126, 134116.
- (29) Neugebauer, J. On the Calculation of General Response Properties in Subsystem Density Functional Theory. J. Chem. Phys. 2009, 131, 084104.
- (30) Pavanello, M. On the Subsystem Formulation of Linear-Response Time-Dependent DFT. J. Chem. Phys. **2013**, 138, 204118.
- (31) Mosquera, M. A.; Jensen, D.; Wasserman, A. Fragment-Based Time-Dependent Density Functional Theory. *Phys. Rev. Lett.* **2013**, *111*, 023001.
- (32) Huang, C.; Libisch, F.; Peng, Q.; Carter, E. A. Time-Dependent Potential-Functional Embedding Theory. J. Chem. Phys. 2014, 140, 124113.

- (33) Krishtal, A.; Ceresoli, D.; Pavanello, M. Subsystem Real-Time Time Dependent Density Functional Theory. J. Chem. Phys. 2015, 142, 154116.
- (34) Krishtal, A.; Pavanello, M. Revealing Electronic Open Quantum Systems with Subsystem TDDFT. J. Chem. Phys. **2016**, 144, 124118.
- (35) De Santis, M.; Belpassi, L.; Jacob, C. R.; Severo Pereira Gomes, A.; Tarantelli, F.; Visscher, L.; Storchi, L. Environmental Effects with Frozen-Density Embedding in Real-Time Time-Dependent Density Functional Theory Using Localized Basis Functions. *J. Chem. Theory Comput.* **2020**, *16*, 5695–5711.
- (36) Goez, A.; Jacob, C. R.; Neugebauer, J. Modeling Environment Effects on Pigment Site Energies: Frozen Density Embedding with Fully Quantum-Chemical Protein Densities.

 Computational and Theoretical Chemistry 2014, 1040–1041, 347–359.
- (37) Neugebauer, J.; Louwerse, M. J.; Baerends, E. J.; Wesolowski, T. A. The Merits of the Frozen-Density Embedding Scheme to Model Solvatochromic Shifts. *J. Chem. Phys.* **2005**, *122*, 094115.
- (38) Höfener, S.; Gomes, A. S. P.; Visscher, L. Solvatochromic Shifts from Coupled-Cluster Theory Embedded in Density Functional Theory. *J. Chem. Phys.* **2013**, *139*, 104106.
- (39) Zbiri, M.; Daul, C. A.; Wesolowski, T. A. Effect of the F-Orbital Delocalization on the Ligand-Field Splitting Energies in Lanthanide-Containing Elpasolites. *J. Chem. Theory Comput.* **2006**, 2, 1106–1111.
- (40) Zbiri, M.; Atanasov, M.; Daul, C.; Garcia-Lastra, J. M.; Wesolowski, T. A. Application of the Density Functional Theory Derived Orbital-Free Embedding Potential to Calculate the Splitting Energies of Lanthanide Cations in Chloroelpasolite Crystals. *Chem. Phys. Lett.* 2004, 397, 441–446.

- (41) Bensberg, M.; Neugebauer, J. Density Functional Theory Based Embedding Approaches for Transition-Metal Complexes. Phys. Chem. Chem. Phys. 2020, 22, 26093–26103.
- (42) Sharifzadeh, S.; Huang, P.; Carter, E. Embedded Configuration Interaction Description of CO on Cu(111): Resolution of the Site Preference Conundrum. J. Phys. Chem. C 2008, 112, 4649–4657.
- (43) Zhao, Q.; Carter, E. A. Revisiting Competing Paths in Electrochemical CO2 Reduction on Copper via Embedded Correlated Wavefunction Theory. J. Chem. Theory Comput. 2020, 16, 6528–6538.
- (44) Genova, A.; Ceresoli, D.; Pavanello, M. Periodic Subsystem Density-Functional Theory.
 J. Chem. Phys. 2014, 141, 174101.
- (45) Fux, S.; Kiewisch, K.; Jacob, C. R.; Neugebauer, J.; Reiher, M. Analysis of Electron Density Distributions from Subsystem Density Functional Theory Applied to Coordination Bonds. Chem. Phys. Lett. 2008, 461, 353–359.
- (46) Schnieders, D.; Neugebauer, J. Accurate Embedding through Potential Reconstruction: A Comparison of Different Strategies. J. Chem. Phys. 2018, 149, 054103.
- (47) Fux, S.; Jacob, C. R.; Neugebauer, J.; Visscher, L.; Reiher, M. Accurate Frozen-Density Embedding Potentials as a First Step Towards a Subsystem Description of Covalent Bonds. J. Chem. Phys. 2010, 132, 164101.
- (48) Banafsheh, M.; Adam Wesolowski, T. Nonadditive Kinetic Potentials from Inverted Kohn–Sham Problem. Int. J. Quantum Chem. 2018, 118, e25410.
- (49) Khait, Y. G.; Hoffmann, M. R. In Annual Reports in Computational Chemistry; Wheeler, R. A., Ed.; Annual Reports in Computational Chemistry; Elsevier, 2012; Vol. 8; pp 53–70.

- (50) Tamukong, P. K.; Khait, Y. G.; Hoffmann, M. R. Density Differences in Embedding Theory with External Orbital Orthogonality. *J. Phys. Chem. A* **2014**, *118*, 9182–9200.
- (51) Chulhai, D. V.; Jensen, L. Frozen Density Embedding with External Orthogonality in Delocalized Covalent Systems. *J. Chem. Theory Comput.* **2015**, *11*, 3080–3088.
- (52) Chulhai, D. V.; Jensen, L. External Orthogonality in Subsystem Time-Dependent Density Functional Theory. *Phys. Chem. Chem. Phys.* **2016**, *18*, 21032–21039.
- (53) Manby, F. R.; Stella, M.; Goodpaster, J. D.; Miller, T. F. A Simple, Exact Density-Functional-Theory Embedding Scheme. J. Chem. Theory Comput. 2012, 8, 2564–2568.
- (54) Tölle, J.; Böckers, M.; Neugebauer, J. Exact Subsystem Time-Dependent Density-Functional Theory. J. Chem. Phys. **2019**, 150, 181101.
- (55) Tölle, J.; Böckers, M.; Niemeyer, N.; Neugebauer, J. Inter-Subsystem Charge-Transfer Excitations in Exact Subsystem Time-Dependent Density-Functional Theory. J. Chem. Phys. 2019, 151, 174109.
- (56) Niemeyer, N.; Tölle, J.; Neugebauer, J. Approximate versus Exact Embedding for Chiroptical Properties: Reconsidering Failures in Potential and Response. J. Chem. Theory Comput. 2020, 16, 3104–3120.
- (57) Baerends, E. J.; Ziegler, T.; Atkins, A. J.; Autschbach, J.; Bashford, D.; Baseggio, O.; Bérces, A.; Bickelhaupt, F. M.; Bo, C.; Boerritger, P. M.; Cavallo, L.; Daul, C.; Chong, D. P.; Chulhai, D. V.; Deng, L.; Dickson, R. M.; Dieterich, J. M.; Ellis, D. E.; van Faassen, M.; Ghysels, A.; Giammona, A.; van Gisbergen, S. J. A.; Goez, A.; Götz, A. W.; Gusarov, S.; Harris, F. E.; van den Hoek, P.; Hu, Z.; Jacob, C. R.; Jacobsen, H.; Jensen, L.; Joubert, L.; Kaminski, J. W.; van Kessel, G.; König, C.; Kootstra, F.; Kovalenko, A.; Krykunov, M.; van Lenthe, E.; McCormack, D. A.; Michalak, A.; Mitoraj, M.; Morton, S. M.; Neugebauer, J.; Nicu, V. P.; Noodleman, L.;

- Osinga, V. P.; Patchkovskii, S.; Pavanello, M.; Peeples, C. A.; Philipsen, P. H. T.; Post, D.; Pye, C. C.; Ramanantoanina, H.; Ramos, P.; Ravenek, W.; Rodríguez, J. I.; Ros, P.; Rüger, R.; Schipper, P. R. T.; Schlüns, D.; van Schoot, H.; Schreckenbach, G.; Seldenthuis, J. S.; Seth, M.; Snijders, J. G.; Solà, M.; M., S.; Swart, M.; Swerhone, D.; te Velde, G.; Tognetti, V.; Vernooijs, P.; Versluis, L.; Visscher, L.; Visser, O.; Wang, F.; Wesolowski, T. A.; van Wezenbeek, E. M.; Wiesenekker, G.; Wolff, S. K.; Woo, T. K.; Yakovlev, A. L. ADF2018, SCM, Theoretical Chemistry, Vrije Universiteit, Amsterdam, The Netherlands, https://www.scm.com (accessed Jan 18, 2018).
- (58) te Velde, G.; Bickelhaupt, F. M.; Baerends, E. J.; Fonseca Guerra, C.; van Gisbergen, S. J. A.; Snijders, J. G.; Ziegler, T. Chemistry with ADF. J. Comput. Chem. 2001, 22, 931–967.
- (59) Goodpaster, J. D.; Barnes, T. A.; Manby, F. R.; Miller, T. F. Density Functional Theory Embedding for Correlated Wavefunctions: Improved Methods for Open-Shell Systems and Transition Metal Complexes. J. Chem. Phys. 2012, 137, 224113.
- (60) Goodpaster, J. D.; Barnes, T. A.; Manby, F. R.; Miller, T. F. Accurate and systematically improvable density functional theory embedding for correlated wavefunctions. *J. Chem. Phys.* **2014**, *140*, 18A507.
- (61) Böckers, M.; Neugebauer, J. Excitation Energies of Embedded Open-Shell Systems: Unrestricted Frozen-Density-Embedding Time-Dependent Density-Functional Theory. J. Chem. Phys. 2018, 149, 074102.
- (62) Casida, M. E. Recent Advances in Density Functional Methods; pp 155–192.
- (63) Vosko, S. H.; Wilk, L.; Nusair, M. Accurate Spin-dependent Electron Liquid Correlation Energies for Local Spin Density Calculations: A Critical Analysis. Can. J. Phys. 1980, 58, 1200–1211.

- (64) Van Lenthe, E.; Baerends, E. J. Optimized Slater-type basis sets for the elements 1–118.

 J. Comput. Chem. 2003, 24, 1142–1156.
- (65) Fermi, E. A Statistical Method for the Determination of Some Atomic Properties and the Application of this Method to the Theory of the Periodic System of Elements. Z. Phys. 1928, 48, 9.
- (66) Franchini, M.; Philipsen, P. H. T.; van Lenthe, E.; Visscher, L. Accurate Coulomb Potentials for Periodic and Molecular Systems through Density Fitting. J. Chem. Theory Comput. 2014, 10, 1994–2004.
- (67) Humbert-Droz, M.; Zhou, X.; Shedge, S. V.; Wesolowski, T. A. How to Choose the Frozen Density in Frozen-Density Embedding Theory-based Numerical Simulations of Local Excitations? *Theor Chem Acc* 2013, 133, 1405.
- (68) Nafziger, J.; Wasserman, A. Density-Based Partitioning Methods for Ground-State Molecular Calculations. J. Phys. Chem. A 2014, 118, 7623–7639.
- (69) Gritsenko, O. V. Recent Progress in Orbital-free Density Functional Theory; Recent Advances in Computational Chemistry; WORLD SCIENTIFIC, 2012; Vol. Volume 6; pp 355–365.
- (70) Huang, C.; Pavone, M.; Carter, E. A. Quantum Mechanical Embedding Theory Based on a Unique Embedding Potential. *J. Chem. Phys.* **2011**, *134*, 154110.
- (71) Huang, C.; Carter, E. A. Potential-Functional Embedding Theory for Molecules and Materials. *J. Chem. Phys.* **2011**, *135*, 194104.
- (72) Cohen, M. H.; Wasserman, A. On the Foundations of Chemical Reactivity Theory. *J. Phys. Chem. A* **2007**, *111*, 2229–2242.
- (73) Elliott, P.; Burke, K.; Cohen, M. H.; Wasserman, A. Partition Density-Functional Theory. *Phys. Rev. A* **2010**, *82*, 024501.

(74) Scholz, L.; Tölle, J.; Neugebauer, J. Analysis of Environment Response Effects on Excitation Energies within Subsystem-Based Time-Dependent Density-Functional Theory.

Int. J. Quantum Chem. 2020, 120, e26213.

TOC Graphic

